

# METHODS FOR SOLVING THE PHASE PROBLEM IN DIGITAL PROCESSING OF IMAGES. PART III. RECONSTRUCTION ALGORITHMS

P.A. Bakut, A.A. Pakhomov, A.D. Ryakhin, and I.P. Plotnikov

*Scientific-Production Union "Astrofizika", Moscow  
Received January 24, 1992*

*Based on a comparative analysis of the well-known approaches to solving the –  
problem sought-for and studied is an algorithm that possesses the best properties.*

*A minimum number of image samplings sufficient for its reconstruction are  
determined. Stability of the algorithm with respect to noise is studied theoretically  
and experimentally. Some results of physical experiments are also given in this paper.*

## RECONSTRUCTION ALGORITHMS

As was shown in Part II analytical solutions of the phase problem are feasible but a narrow class of images and, in particular, for those that have a point source in their intensity distribution.<sup>11</sup>

Among the methods for solving the phase problem there are methods of direct solution of the phase problem based on numerical solutions of the autocorrelation equation (see Part I, Eq. (4)). An algorithm for reconstructing the intensity-quantized images considered in Ref. 2 is, in fact, reduced to a successive looking over all possible solutions with rejection of extraneous ones. Using this approach in Ref. 2 they succeeded, in reconstruction only true solutions of all, without any exceptions, solutions. However, the procedure of seeking for all solutions is too complicated and takes a lot of computer time. Thus, for instance, the processing of an array of 25×25 6 bit pixels of an image took about 2.5 hours of BESM-6 computer time. In Ref. 3 one can find a modification of this algorithm for the case of nonquantized images, which also takes a lot of computer time.

Some theoretical algorithms<sup>4,5</sup> can be feasible based on seeking for  $z$ -transform of the autocorrelation  $R_Q(z_1, z_2) = R_f(z_1, z_2)R_f(z_1^{-1}, z_2^{-1})$ , with the following calculation of roots  $R_Q$  with respect to each variable and on solution of a system of linear equations for the coefficients of the polynomials  $R_f(z)$  and  $R_f(z^{-1})$ . The main deficiency of these algorithms is difficult and cumbersome factorisation of two-dimensional determination polynomials as well as significant errors of the root in presence of noise.

More realistic could be algorithms that are based on iteration solution of the autocorrelation equation. The principle of operation of these algorithms is as follows. Let  $J^k(\mathbf{n})$  be the estimate of an image, and  $Q^k(\mathbf{n})$  be the corresponding estimate of the autocorrelation, then the discrepancy between this estimate and true autocorrelation can be given by

$$\Delta Q^k(\mathbf{n}) = \sum_{\mathbf{n}} |Q^k(\mathbf{n}) - Q(\mathbf{n})|^2 = \|Q^k - Q\| .$$

The estimate  $J^k(\mathbf{n})$  is then varied so that the value  $\Delta Q^k(\mathbf{n})$  is reduced to minimum.

The minimization of  $\Delta Q^k(\mathbf{n})$  could be done by different methods. Thus in Ref. 6 it was done using the Monte Carlo method, while in Refs. 7 and 8 the gradient methods were used. The first disadvantage of these algorithms is their

cumbersome character what limits their applicability only to few-dimensional images, and the second disadvantage is caused by existence of many extrema in the  $\Delta Q^k(\mathbf{n})$  behavior. The function  $\Delta Q^k(\mathbf{n})$  depends on  $(N_1 + 1)(N_2 + 1)$  variables determined within the image region.

Such functions have commonly many local extrema in addition to the global one. As a result, one can reach a global extremum only after looking through all local extrema the number of which are unpredictable and are determined both by the view of the functional and by the image itself.

One more algorithm of approximate solution of the problem<sup>9,10</sup> is worth noting here. To perform this algorithm one should take a sampling of the module values twice as dense as is needed according to Kotel'nikov theorem. This can be done by putting the autocorrelation into the zeroth data array with the dimensions twice as big as the dimensions of the autocorrelation and then making an ordinary discrete Fourier transform. Then, assuming that the module values at each excess point depend only on two values at the nearest basic points of sampling one can determine differences of phases of the form  $\Delta\varphi_k = |\varphi_{k,l} - \varphi_{k+1,l}|$ ,  $\Delta\varphi_l = |\varphi_{k,l} - \varphi_{k,l+1}|$ . Then an estimate of the phase itself is constructed by joining  $\Delta\varphi_k$  and  $\Delta\varphi_l$  and making use of the circumstance that the final value of the phase is independent of the approach ways.

Despite the indefiniteness of the phase difference sign and the need for solution trials, in a two-dimensional case only true solutions have been reconstructed (what confirms the important role of the closeness condition once more). A deficiency of the algorithm is its low accuracy caused by rough approximation of the module value. However, this algorithm well suits the construction of the initial estimate to be used in the iteration technique considered below.

## ITERATION ALGORITHMS

1. *Optimal algorithm.* From the authors' point of view the iteration algorithms that are modifications of the Gerchberg-Saxton<sup>11</sup> algorithm are most promising for solving the problem under consideration.

Briefly, the algorithm operation can be represented by the scheme

$$J_{k+1} = \hat{P}_1 \hat{P}_2 \hat{P}_3 J_k , \quad (1)$$

where  $J_k$  is the image estimate at the  $k$ th iteration,  $\hat{P}_1$  is the operator of projection onto the set of positive functions,  $\hat{P}_2$  is the operator of projection onto the set of finite functions (defined within the region  $S$ ), and  $\hat{P}_3$  is the operator of projection onto the set of functions with a preset absolute value of their Fourier spectra. From the definition of the projection operator<sup>12</sup> one can directly find the form of the operators  $\hat{P}_1$  and  $\hat{P}_2$

$$\hat{P}_1 I = \begin{cases} I(\mathbf{n}) & \text{at } I(\mathbf{n}) \geq 0, \\ 0 & \text{at } I(\mathbf{n}) < 0, \end{cases} \quad \hat{P}_2 I = \begin{cases} I(\mathbf{n}) & \text{at } \mathbf{n} \in 0, \\ 0 & \text{at } \mathbf{n} \notin 0, \end{cases} \quad (2)$$

where  $I(\mathbf{n})$  is an arbitrary real function. Let us now find the view of the operator  $\hat{P}_3$ . Let  $f(\mathbf{x}) = |f(\mathbf{x})| \exp\{i\varphi(\mathbf{x})\}$  be an arbitrary Fourier spectrum, and  $g(\mathbf{x}) = A(\mathbf{x}) \exp\{i\varphi(\mathbf{x})\}$  be the Fourier spectrum with a preset module  $A(\mathbf{x})$ . Let us now find a relationship between  $\varphi(\mathbf{x})$  and  $\psi(\mathbf{x})$ . According to definition of the projection operator we have

$$\|f - \hat{P}_3 f\|^2 = \|f - g\|^2 = \sum_x \{|f(\mathbf{x})|^2 + A^2(x) - 2|f(\mathbf{x})| A(x) \cos[\varphi(\mathbf{x}) - \psi(\mathbf{x})]\} = \min.$$

Minimum of this function is attained at  $\varphi(\mathbf{x}) = \psi(\mathbf{x})$  and  $|f(\mathbf{x})| = A(\mathbf{x})$ . Therefore the operator  $\hat{P}_3$  takes the form

$$\hat{P}_3 J_k = \tilde{J}_k(\mathbf{x}) \frac{A(\mathbf{x})}{|\tilde{J}_k(\mathbf{x})|}, \quad (3)$$

where  $\tilde{J}_k(\mathbf{x}) = \hat{F}\{J_k\}$ ,  $\hat{F}$  is the Fourier transform operator,  $A(\mathbf{x})$  is the preset module of the Fourier spectrum.

Since any *a priori* information (limitations) can be interpreted as closed sets, reconstructing algorithm (1) can be reduced to a successive projecting onto these sets and seeking for a cross element. Normally, analysis of such algorithm convergences is based on the statement<sup>12</sup> that states the convergence to a true solution provided that the sets corresponding to operators  $\hat{P}_1$  and  $\hat{P}_2$  are convex.

However the set corresponding to operator  $\hat{P}_3$  is not convex. For this reason it is necessary to study its convergence in more detail. A theoretical analysis<sup>13</sup> shows that the error decreases in the course of the reconstruction that means that the algorithm converges. As the experimental studies have shown the algorithm converges quite rapidly during 10–30 iterations and then the convergence sharply decreases and by 50–60 iterations it reaches a saturation level which is practically the same during the following 2–10 thousand iterations and more (see Fig. 1a).

In other words the estimate of an image becomes independent of the iteration number and the standard deviation from a true image becomes frozen somewhere at 10–15 percent. This disadvantage makes us to seek for ways to overcome stagnation of algorithm (1) which we shall call optimal because the correction of images in it is performed with the projection operators, i.e., optimally, in the sense of norm.

**2. Shaking algorithm.** The below-considered algorithms based on the input control have been proposed by Fienup,<sup>13</sup> and while they are not strictly proved, their use allows one to overcome stagnation of algorithm (1). Let us now consider the functioning of the nonlinear operator  $\hat{P}_3$ . It is obvious that small perturbations at its input result in small perturbations at its output. Since the output is the estimate  $I_k(\mathbf{n})$  that does not satisfy *a priori* limitations imposed on images. Let us formulate the problem: to give at the input at the next iteration cycle, such an estimate  $J_{k+1}(\mathbf{n})$  to obtain at the output the estimate  $I_{k+1}(\mathbf{n})$  that would satisfy the *a priori* limitations. It is natural to assume that in this case the input variation should have the form

$$\Delta J_k(\mathbf{n}) = \begin{cases} 0, & \mathbf{n} \in \Gamma_k, \\ -I_k(\mathbf{n}), & \mathbf{n} \notin \Gamma_k, \end{cases}$$

where  $\Gamma_k$  is the region in which  $I_k(\mathbf{n}) \geq 0$  and  $\mathbf{n} \in S$ . Then in the general case we have for  $J_{k+1}(\mathbf{n})$

$$J_{k+1}(\mathbf{n}) = J_k(\mathbf{n}) + \beta \Delta J_k(\mathbf{n}) = \begin{cases} J_k(\mathbf{n}), & \mathbf{n} \in \Gamma_k, \\ J_k(\mathbf{n}) - \beta I_k(\mathbf{n}), & \mathbf{n} \notin \Gamma_k, \end{cases} \quad (4)$$

where  $\beta \in (0, 1)$ . One can also try to compensate for a distortion in the region of image at the input considering the estimate  $I_k(\mathbf{n})$  as an input. As a result we have

$$J_{k+1}(\mathbf{n}) = I_k(\mathbf{n}) + \beta \Delta J_k(\mathbf{n}) = \begin{cases} I_k(\mathbf{n}), & \mathbf{n} \in \Gamma_k, \\ J_k(\mathbf{n}) - \beta I_k(\mathbf{n}), & \mathbf{n} \notin \Gamma_k. \end{cases} \quad (5)$$

A combination of these methods leads to the third relation for input

$$J_{k+1}(\mathbf{n}) = \begin{cases} I_k(\mathbf{n}), & \mathbf{n} \in \Gamma_k, \\ J_k(\mathbf{n}) - \beta I_k(\mathbf{n}), & \mathbf{n} \notin \Gamma_k. \end{cases} \quad (6)$$

Thus, one can see that algorithms (4), (5), and (6) differ from optimal only by corrections in the image region. As was experimentally shown algorithms (4) and (5) converge even more slowly than the optimal one. On the other hand, algorithms (6), which we shall call the shaking algorithm, has a very interesting behavior. First of all, the estimate of the image  $J_{k+1}(\mathbf{n})$  does not satisfy the *a priori* limitations. Second, the errors first fall off very rapidly with growth of the iteration number, but then decrease slows down and after 100–500 iterations the errors again sharply decrease down to 0.1–0.01 percent level. And for the third, the convergency of this algorithm strongly depends on the value of the constant  $\beta$ . For example, at  $\beta \geq 1$  the algorithm diverges. An optimal, i.e., providing most rapid convergence, value of  $\beta$  from the interval (0, 1) depends on a concrete view of the image to be reconstructed.

The main deficiency of the shaking algorithm is its general instability, i.e., there can occur an unpredictable growth of errors (see Fig. 1b).

**3. A combined algorithm.** A natural generalization of the above algorithms could be their alternative use aimed both at compensation for instability of the shaking algorithm and for stagnation of the optimal algorithm.

Let a combined algorithm be given by

$$J_{k+1}(\mathbf{n}) = \begin{cases} I_k(\mathbf{n}), & \mathbf{n} \in \Gamma_k, \\ \alpha\{J_k(\mathbf{n}) - \beta I_k(\mathbf{n})\}, & \mathbf{n} \notin \Gamma_k. \end{cases} \quad (7)$$

At  $\alpha = 0$  this expression gives the optimal algorithm,

while at  $\alpha = 1$  it represents the shaking algorithm. The simplest version of the combined algorithm is

$$\{K_1 \text{ iterations at } \alpha = 0 + L_1 \text{ iterations at } \alpha = 1\} \times \\ \times M_1 + K \text{ iterations at } \alpha = 0. \quad (8)$$

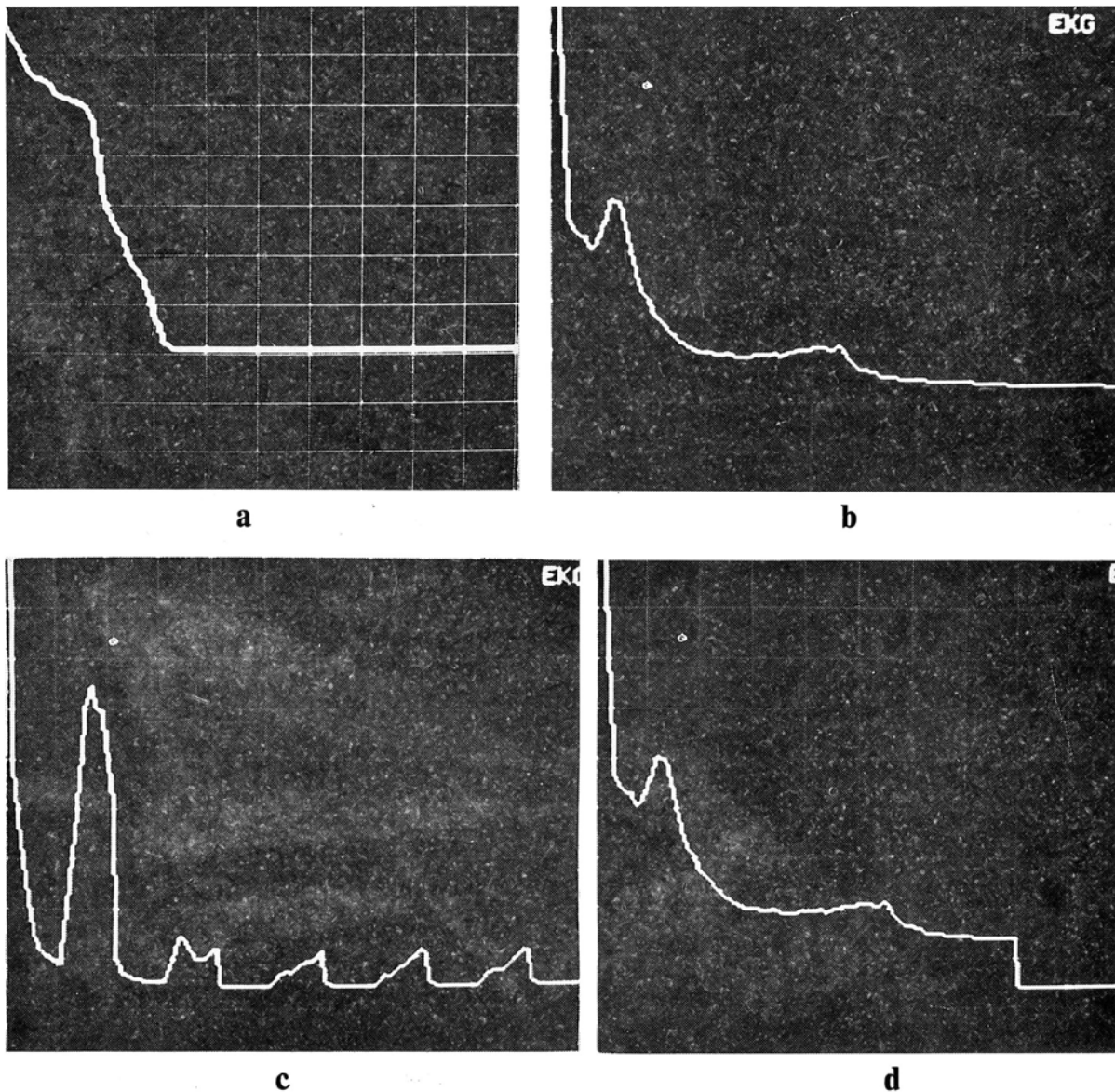


FIG. 1. Dependence of the image reconstruction error on the iteration number when using: a) optimal algorithm, b) shaking algorithm, c) alternating the optimal and shaking algorithms each 10 iterations, and d) optimal algorithm after 80 iterations of the shaking algorithm.

It should be noted that an intermediate version is feasible with  $\alpha \in (0, 1)$ . However, the experimental modeling has shown such an algorithm has a slower convergence compared to that of the combined algorithm (its convergence is approximately as that of the optimal one, though the stagnation occurs later).

In order to determine the parameters  $K_1$ ,  $L_1$ ,  $M_1$ , and  $\beta$ , that provide the most rapid convergence of the combined algorithm we have studied it experimentally. First we sought for an optimal  $\beta$  value (by taking and substituting 3–4 values

from the interval  $(0, 1)$ , and then at a fixed  $\beta$  value we studied the convergence at different values of  $K_1$ ,  $L_1$ , and  $M_1$ . Finally, it appeared that the best quality of reconstruction occurred with the combination of the parameters  $K_1 = L_1 = 10$  at  $M_1 = 1, 2$ , and 3.

Behavior of errors during the course of the combined-algorithm work looks a little bit unusual. Thus, at  $\alpha = 0$  the errors decrease, then at  $\alpha = 1$  the errors increase, and the next change for optimal algorithm ( $\alpha = 0$ ) again results in a

decrease of errors but now down to a level, which is lower than at the previous stage (see Fig. 1c). Thus it is obvious that the use of shaking ( $\alpha = 1$ ) enables one to overcome the stagnation of the optimal algorithm. A cyclic alternation of these two algorithms can finally result in errors as low as  $10^{-4}$  to  $10^{-6}$ .

Good results can be obtained when using the combined algorithm at  $M_1 = 1$ . In this case first 100–150 iterations ( $L_1$ ) are performed with  $\alpha = 1$ , then 20–30 iterations ( $K_1$ ) are performed with  $\alpha = 0$  (see Fig. 1d). The final errors of this algorithm are close to those of the combined algorithm.

It is interesting to note one peculiar feature. As was shown in Part I, the phase problem has a unique solution accurate to equivalence, what means that in practice image reconstruction yields two images, i.e., an actual one and its analog turned about. The algorithm can converge to either of the solutions depending on the initial estimate. However the shaking ( $\alpha = 1$ ) can change orientation of an image and the reconstruction algorithm starts to converge to the opposite solution. Sometimes, though very seldom, a situation can happen when two solutions (the true and the reversed) overlap. In this case it is impossible to reconstruct the image and one simply needs for reiteration of the whole cycle of the image reconstruction but using a new initial estimate.

The problem on choosing the initial estimates we have studied especially. We took the initial estimates with the true module of the spectrum and zero or random phase, the estimates uniformly distributed over the  $S$  region alone and over the whole array, therefore just this type of the initial estimate was used in all experiments.

An image size ( $S$  region) was determined at a threshold filtration of the autocorrelation at the level 0.1 of its maximum value. Thus obtained region of autocorrelation exceeded the image region  $S$  by a factor of 1.5–1.8. As modeling has shown a 10 percent underestimation of  $S$  makes the algorithm inoperative. On the other hand, at the overestimation of  $S$  by a factor below 1.5 the algorithm still works but the number of iterations increases 5–6 times. It should be noted that the use of this algorithm gives the best results when applied to reconstruction of compact images without a fine structure and dissected contour. Therefore for reconstructing more complicated images it is necessary to use the abundance of the spectrum module for the image size not larger than a quarter of the whole field.

**MINIMUM NUMBER OF THE MODULE SAMPLINGS AND ANALYSIS OF A RECONSTRUCTION ALGORITHM STABILITY TO NOISE**

In practice of reconstructing images the spectrum module is known at a finite number of sampling points. Unambiguity of the image reconstruction in such a situation has been analyzed and proved in Ref. 14. As follows from this reference an unambiguous reconstruction of an image of  $(N_1 + 1)(N_2 + 1)$  size can be done, in general, if the spectrum module is known at  $(2N_1 + 1)(2N_2 + 1)$  sampling points. Since the module of the spectrum of a real image is an even function it is sufficient to know only a half of its value. Moreover, taking into account the energy

normalization relation  $\left(\sum_{\mathbf{n}} J(\mathbf{n}) = 1\right)$  one finds the number of samplings sufficient for image reconstruction as  $L = 2N_1N_2 + N_1 + N_2$ . However, the general number of independent image samplings, with the account of normalization, is  $N_1N_2 + N_1 + N_2$ , what gives an idea that

$L$  number is not minimum. To determine the minimum number of the module samplings let us again make use of the method of reducing a discrete two-dimensional case to a one-dimensional case.

Let us stretch the image  $J(n_1, n_2)$  line by line and omitting zero lines thus reducing it to a one-dimensional image  $T(n)$  according to the rule

$$T_n = J_{n_1, n_2} \text{ where } n = n_1 + n_2(N_1 + 1).$$

As a result, corresponding to  $T(n)$  the one-dimensional autocorrelation  $Q_l$  is (see Part I)

$$Q_l = Q_{l_1, l_2} + Q_{N_1 - l_1 - 1, l_2 + 1},$$

where  $Q_{l_1, l_2}$  is the two-dimensional autocorrelation of the image  $J(n_1, n_2)$ . Total number of elements of the one-dimensional autocorrelation  $Q_l$  is  $2(N_1N_2 + N_1 + N_2) + 1$ . The size of region the one-dimensional image  $T(n)$  is  $0 \leq n \leq N_1N_2 + N_1 + N_2$ , and the size of the one-dimensional grid, on which the module  $|F\{T\}|$  of the spectrum is defined is  $2(N_1N_2 + N_1 + N_2) + 1$ . Taking this as well as the normalizing relation and the fact that the spectrum modulus is even into account one finds that the minimum number of the modulus samplings sufficient for determination of the two-dimensional image  $J(n_1, n_2)$  is  $L_{\min} = N_1N_2 + N_1 + N_2$ . In addition, one obtains a restriction imposed on the maximum size  $K$  of the image that could be reconstructed using data on modulus defined by an array of the length  $M$ .

Let the image and the array be quadratic and  $N_1 + 1 = N_2 + 1 = K$ , and  $M$  be the size of the arrays describing the Fourier and image planes. The number of independent samplings of the modulus is  $M^2/2$  and it should involve the minimum number of samplings, i.e.,  $L_{\min} \leq M^2/2$ . As a result the maximum size of the image is given by

$$K_{\max}^2 - 1 \leq \frac{M^2}{2} \text{ and } K_{\max} \leq \frac{2}{3} M.$$

But in practice it is advisable to take  $K$  from the interval  $M/4 - M/2$  in order to obtain a faster convergence.

Let us now consider the stability of algorithms in presence of noise. In the one-dimensional case the following statement is valid.<sup>15</sup> For a one-dimensional, real, and symmetric succession is autocorrelation (i.e., it obeys Eq. (5) from Part I) it is necessary and sufficient that its Fourier spectrum is positive.

Unfortunately, this statement cannot be generalized on the two-dimensional case and, moreover, in the latter case quite opposite statement is valid.

*Statement.* The Lebesgue measure of the subset of the autocorrelation  $\{Q_{n_1, n_2}\}$  from the set of all real and symmetric successions  $\{B_{n_1, n_2}^0\}$  possessing positive Fourier spectrum is equal to zero.

*Proof.* The set of the real and symmetric successions

$$B_{n_1, n_2}: \{B_{n_1, n_2} = B_{-n_1, -n_2}; -N_1 \leq n_1 \leq N_1, -N_2 \leq n_2 \leq N_2\}$$

is defined by the  $2N_1N_2 + N_1 + N_2 + 1$  independent parameters. Let us now separate out from this set a subset

$\{B_{n_1, n_2}^0\}$  that differs from it only by the values of central elements, which we define as follows:

$$B_{0,0}^0 \geq 2 \sum_{-N_1}^{N_1} \sum_{-N_2}^{N_2} |B_{n_1, n_2}|.$$

In this case the Fourier transform  $F\{B_{n_1, n_2}^0\} = f_{B^0}(x_1, x_2)$  is given by

$$f_{B^0}(x_1, x_2) = B_{0,0}^0 + 2 \sum_{-N_1}^{N_1} \sum_{-N_2}^{N_2} B_{n_1, n_2} \cos(n_1 x_1 + n_2 x_2).$$

From the construction of  $B_{n_1, n_2}^0$  it follows that  $f_{B^0}(x_1, x_2) \geq 0$  for arbitrary values of  $x_1$  and  $x_2$ . The number of independent parameters of the set  $B_{n_1, n_2}^0$  is  $2N_1 N_2 + N_1 + N_2$ .

At the same time the number of independent parameters of the set of autocorrelations coincide with the number of the image parameters (because it must satisfy Eq. (5) from Part I) and is equal to  $(N_1 + 1)(N_2 + 1) < 2N_1 N_2 + N_1 + N_2$  at  $N_1, N_2 > 1$ . Therefore, according to Statement 1 (Part I) the Lebesgue measure of the subset autocorrelations from the set of all real and symmetric successions with the positive center is equal to zero.

This enables one to draw a qualitative conclusion that the two-dimensional autocorrelation (in contrast to the two-dimensional case) is a very specific succession. Thus, for example, an infinitely small noise component will, as a rule, transform this succession into another succession which is not now the autocorrelation.

In this sense the two-dimensional phase problem is unstable, i.e., a noise makes it impossible to obtain an exact solution.

However, numerous experiments have shown that there always exists an approximate solution—image whose autocorrelation is very close to a noisy autocorrelation succession while it itself is close the true image.

Just this property (experimental observation) indirectly confirms the validity of using the above-chosen iteration technique of reconstruction that enables one to obtain an approximate solution when the exact one is unvaliable.

In connection with the above said the question on errors of reconstruction arises quite naturally. Using Eq. (5) (Part I) one can readily obtain a rough qualitative estimate of errors in the image reconstruction at a preset error in autocorrelation (or the square modulus)  $\delta_j = \sqrt{\delta_Q}$ .

Thus, in Ref. 16 one can find a theoretical calculations of this dependence using Cramer-Rao inequality, where the phase problem was considered as a problem on reconstructing a complex Gaussian field from the intensity of its spectrum.

Experimental investigation of the noise characteristics of the phase problem used two types of noise:

Multiplicative

$$A^2(\mathbf{x}) = A_0^2(\mathbf{x})\{1 + g \cdot n(\mathbf{x})\} \tag{9}$$

and additive

$$A^2(\mathbf{x}) = A_0^2(\mathbf{x}) + g \cdot n(\mathbf{x}), \tag{10}$$

where  $A(\mathbf{x})$  and  $A_0(\mathbf{x})$  are the distorted and undistorted amplitudes of spectra, respectively;  $g$  is a changeable constant,  $n(x)$  is the Gaussian process with nonzero mean value and unit variance. In the former an error in the modulus was introduced as follows:

$$\delta_1 = \left\langle \frac{\sum_x A_0^2(\mathbf{x}) \{\sqrt{1 + gn(\mathbf{x})} - 1\}^2}{\sum_x A_0^2(\mathbf{x})} \right\rangle,$$

and in the latter

$$\delta_2 = \left\langle \frac{\sum_x A_0^2(\mathbf{x}) \left\{ \sqrt{1 + \frac{gn(\mathbf{x})}{A_0^2(\mathbf{x})}} - 1 \right\}^2}{\sum_x A_0^2(\mathbf{x})} \right\rangle.$$

Then we studied a normalized rms error over the image  $\delta$  of the reconstructed image from the true one at the moment of finishing the reconstruction procedure. In both cases the dependence of  $\delta$  on  $\delta_1$  and  $\delta_2$  is practically the same. Thus, at a low noise ( $10^{-6} \leq \delta_1$  and  $\delta_2 \leq 10^{-3}$ )  $\delta$  is directly proportional to  $\delta_1$  and  $\delta_2$  (if considered separately). At  $10^{-3} \leq \delta_1$  and  $\delta_2 \leq 10^{-2}$  we also have proportionality between  $\delta$  and  $\delta_1$  and  $\delta_2$  but the proportionality factors are different ( $\delta = 4\delta_1$ ,  $\delta = 3\delta_2$ ). At  $10^{-2} \leq \delta_1$  and  $\delta_2 \leq 0.2$  the value  $\delta$  is approximately proportional to square roots of  $\delta_1$  and  $\delta_2$  ( $\delta = \sqrt{\delta_1}$ ,  $\delta = \sqrt{\delta_2}$ ).

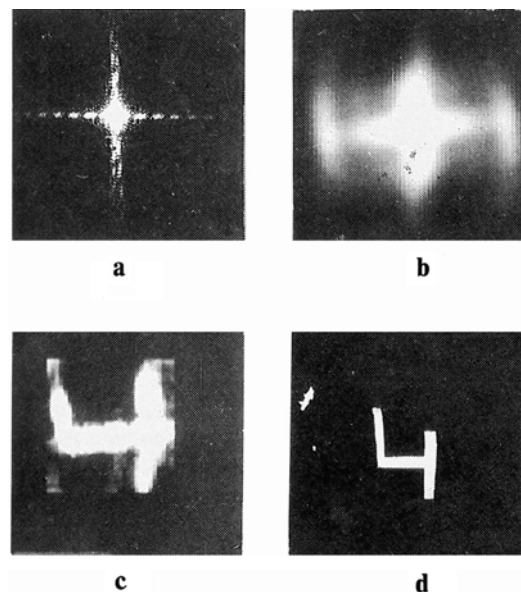


FIG. 2.

To study the stability of the problem solution to the influence of nonlinear noise of a photosensitive emulsion the authors have conducted a very simple physical experiment. A plane optical wave formed by collimating a He-Ne-laser radiation beam ( $\lambda = 0.63 \mu\text{m}$ ) has been transmitted through a mask (in the form of figure 4). A collecting lens with

$F = 500 \mu\text{m}$  then performed the Fourier transform of the transmitted radiation. The intensity of radiation at the focus of this lens was then recorded with an ordinary camera. With the size  $l$  of the mask a resolution element of such a system in the Fourier plane is  $\Delta = \lambda F/l$ . In order to reconstruct the autocorrelation the intensity of the spectrum should be digitized with the step  $d$ , which must be twice as small as the resolution element ( $d \leq \lambda F/2l$ ).

To digitize the spectrum we used an R-1700 instrumental complex that provides a  $50 \mu\text{m}$  digitization increment. Since  $l \leq \lambda F/2l \approx 3.15 \mu\text{m}$  the mask size  $l$  was taken to be 3 mm.

Thus recorded on a negative film the module of the Fourier spectrum (see Fig. 2a) was digitized (its intensity) and reduced to an array  $64 \times 64$  elements. This array was then read out to a computer. In the computer we then passed from optical densities and intensities using a procedure of matching the film contrast to provide most sharp boundaries of the autocorrelation.

The reconstructed autocorrelation and image (after 30th iteration) are shown in Fig. 2b and c, respectively, while Fig. 2d shows the true image recorded with a coherent technique and instrumentation.

## REFERENCES

1. P.A. Pavlova, V.N. Pauk, and V.V. Teterin, Tr. S.I. Vavilov State Optical Institute, Leningrad, **70**, No. 204, 55 (1988).
2. A.A. Demin, Radiotekh. Elektron. **28**, No. 10, 2023 (1983).
3. M.A. Fiddy and H.M. Berenyi, Opt. Comm. **59**, 342 (1986).
4. D. Izraelevits and J.S. Lim, ICCASP **35**, 51 (1987).
5. R.A. Gonsalves, SPIE **528**, 20 (1985).
6. M. Nieto-Vesperinas and J.A. Mendes, Opt. Comm. **59**, 249 (1986).
7. V.P. Bakalov, Radiotekh. Elektron. **30**, No. 8, 1565 (1985).
8. M. Nieto-Vesperinas, Opt. Acta **33**, 713 (1986).
9. R.H.T. Bates and K.L. Garden, Optik **61**, 247 (1982).
10. R.H.T. Bates and K.L. Garden, ibid. **62**, 131 (1982).
11. R.W. Gerchberg and W.O. Saxton, ibid. **35**, 237 (1972).
12. D.C. Youba and H. Webb, IEEE Trans. Med. Imaging **1**, 81 (1982).
13. J.R. Fienup, Appl. Opt. **21**, No. 15, 2758 (1982).
14. M.H. Hayes, IEEE Trans. Acoust. Speech. Sign. Proc. **30**, 140 (1982).
15. P.A. Bakut, A.A. Pakhomov, A.D. Ryakhin, K.N. Sviridov, and N.D. Ustinov, Dokl. Akad. Nauk SSSR **290**, 89 (1986).
16. J.N. Cederquist and C.C. Wackerman, J. Opt. Soc. Am. **4**, 1 (1987).